Sn-ZSM-12, a new, large pore MTW type tin-silicate molecular sieve: synthesis, characterization and catalytic properties in oxidation reactions

N.K. Mal, A. Bhaumik, R. Kumar and A.V. Ramaswamy [1]

National Chemical Laboratory, Pune 411 008, India

Received 31 January 1995; accepted 19 April 1995

A new large pore tin-silicate analogue of zeolite ZSM-12 (MTW topology) with Si/Sn molar ratio > 70 has been synthesized hydrothermally using a new template, hexamethylene bis(benzyl dimethyl ammonium hydroxide). This material exhibits an expansion in unit cell volume (XRD), an IR band at 970 cm^{-1} and a charge transfer band at 205 nm in the UV-Vis region indicating the presence of Si–O–Sn units with Sn^{4+} centers in T_d configuration. Sn-ZSM-12 catalyzes the oxidation of phenol, *m*-cresol and *m*-xylene using dilute H_2O_2 as an oxidizing agent.

Keywords: tin-silicate zeolite; Sn-ZSM-12; high silica molecular sieve; Sn-molecular sieve; oxidation catalysts with Sn; selective oxidation reactions

1. Introduction

The incorporation of various tetra- or penta-valent metal ions, such as Ti^{4+}, Ge^{4+} and V^{5+} in crystalline, microporous silicate networks of MFI, MEL and MTW types is known to impart interesting oxidation properties in them. The hydrothermal synthesis of Sn-silicate molecular sieves with MFI (ZSM-5) structures has been claimed in the patent literature [1,2]. Recently, we reported the synthesis of Sn-incorporated in MFI [3] and MEL [4] framework structures, with well-dispersed Sn^{4+} ions, which were capable of catalyzing hydroxylation of phenol and toluene with aqueous H_2O_2. This report describes, for the first time, the synthesis of a large pore tin-silicate analogue of ZSM-12 (MTW topology, consisting of unidimensional channels with 12-membered ring pore openings of 5.7 × 6.1 Å in size) [5] using a new template. These Sn-silicates were characterized through various techniques (XRD, FT-IR, UV-Vis and adsorption). Their catalytic property in the oxidation of organic substrates such as phenol, *m*-cresol and the bulkier *m*-xylene in presence of aqueous H_2O_2 is demonstrated.

---

[1] To whom correspondence should be addressed.

© J.C. Baltzer AG, Science Publishers

2. Experimental

Recently, we have reported the use of a new organic template prepared in our laboratory, viz., 1,6-hexamethylene bis(benzyl dimethyl ammonium hydroxide) for synthesizing ZSM-12 and V-ZSM-12 molecular sieves [6]. The same template was used in the current study. In a typical preparation, 0.46 g of $SnCl_4 \cdot 5H_2O$ (98%, Loba Chemie) in 10 g H_2O was added to 21.0 g of tetraethyl orthosilicate (98%, Aldrich) (TEOS) with stirring. Next, 34.5 g of the organic template (15%, aqueous) was added under vigorous stirring. The entire mixture was stirred for 75 min and then, 0.39 g NaOH dissolved in 14 g of deionized water was added to the resultant clear solution and stirred for another 30 min. The clear solution (pH = 11.7) was charged into a stainless steel autoclave and heated at 433 K under static condition for 5 days to complete the crystallization. After crystallization, the product was filtered, washed with deionized water, dried at 383 K for 5 h and calcined at 793 K for 12 h. The product yield based on the initial input was between 75 and 85 mass%. Three such Al-free Sn-ZSM-12 (MTW structure) samples with Si/Sn input ratios of 75, 100 and 180 (total Sn per unit cell in the calcined samples, A, B and C = 1.26, 0.95 and 0.53, respectively) were prepared. The molar gel composition of the Sn-silicate samples on anhydrous basis was found to be: $0.133R : 1.0SiO_2 : 0.013\text{–}0.003SnO_2 : 0.05Na_2O : 30H_2O$, where R is 1,6-hexamethylene bis(benzyl dimethyl ammonium hydroxide). For comparison, a pure silica polymorph of ZSM-12 (Si-ZSM-12, sample D) and a Sn-impregnated Si-ZSM-12 sample were also prepared. The latter was prepared through the impregnation of Si-ZSM-12 with a $SnCl_4$ solution followed by calcination at 793 K. The Na-form of Sn-ZSM-12 was converted into H-form by the usual ion-exchange procedure [7].

The calcined samples were characterized by XRD, FT-IR, DR-UV-Vis, ^{119}Sn MAS-NMR and sorption techniques [3,4]. The oxidation reactions were carried out batchwise at 353 K over a Sn-ZSM-12 (Si/Sn = 73) sample with a substrate to H_2O_2 mole ratio of 3. Other details of the reaction and analysis of the products are given elsewhere [4].

3. Results and discussion

3.1. PHYSICO-CHEMICAL CHARACTERIZATION

The powder XRD profiles (recorded in a Rigaku D Max III VC instrument using a Cu target) of the Sn-samples resemble that of the Sn-free Si-ZSM-12 (MTW) structure [5] and are free from individual SnO_2, SiO_2 or other impurity phases (fig. 1). The XRD peaks of Sn-free Si-ZSM-12 are slightly more narrow and sharp compared to those of the Sn-containing samples. The crystallinity of the Sn-ZSM-12 samples was estimated to be about 90%, in comparison to the Sn-free Si-ZSM-12. Table 1 shows that the unit cell volume of the Sn-ZSM-12 samples increases with increasing Sn atoms per unit cell. The X-ray photoelectron spectra (VG Scien-

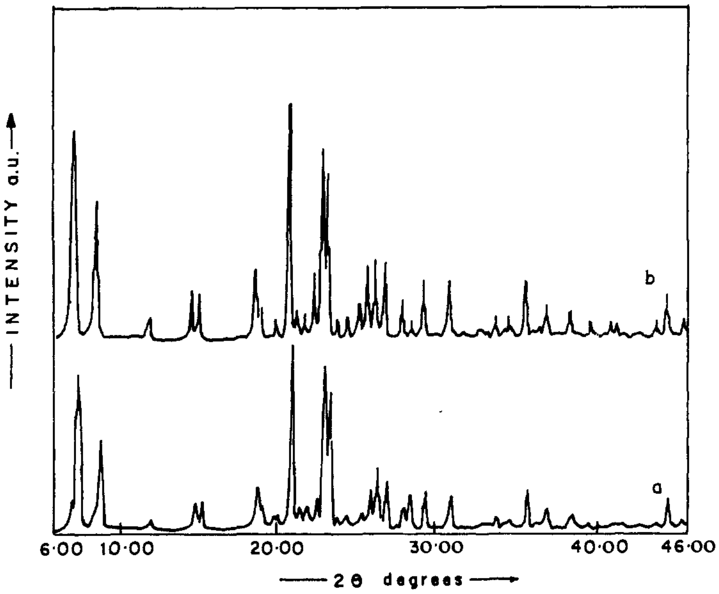

Fig. 1. Powder XRD patterns of Sn-ZSM-12 (a) (Si/Sn mole ratio = 73) and Sn-free Si-ZSM-12 (b) samples.

tific ESCA-3-MK 2 electron spectrometer with Al Kα ray source) showed doublets for the Sn $3d_{3/2}$ and $3d_{5/2}$ electrons with binding energies of 495.9 and 487.3 eV, respectively, confirming the presence of Sn^{4+} on the surface. A binding energy of 285 eV for the C 1s level was used as an internal standard. The values of the surface (XPS) and the bulk compositions (calculated from the chemical analysis using ICP instrument) of the samples given in table 1, are quite comparable and indicate a uniform distribution of Sn^{4+} in the samples. Irrespective of its location in the silicalite framework, this accounts for the observed increase in the unit cell volume (Shannon ionic radii, 0.55 Å for Sn^{4+} and 0.26 Å for Si^{4+}).

Table 1
Physico-chemical characterization of Sn-ZSM-12

Sample	Si/Sn mole ratio			V_{uc} (Å^3)	Sorption capacity[a] (wt%)				Surface area (m^2 g^{-1})
	gel	solid (ICP)[b]	solid (ESCA)		H_2O	cyclo-hexane	n-hexane	mesitylene	
A	75	73	67	1453	8.9	12.2	9.8	3.5	321
B	100	98	95	1447	8.3	12.0	9.6	3.3	310
C	180	177	177	1435	7.5	11.1	8.9	3.0	301
D	∞	–	–	1423	4.9	10.5	8.2	2.7	280

[a] Gravimetric adsorption at $p/p_0 = 0.5$ and at 298 K.

[b] Calcined product, bulk composition by chemical analysis.

The framework IR spectra of the Sn-ZSM-12 samples (in KBr pellets, Nicolet) (fig. 2) show a shoulder around 970 cm^{-1}, in addition to other vibrations associated with the ν_{T-O-T} (1100 cm^{-1}), stretching and bending modes of isolated SiO_4 tetrahedra (1200–1050, 750–850 and 450 cm^{-1}). The band at 960–970 cm^{-1} observed in many Ti-, V-, Mo- and Sn-silicates is a subject of much discussion [8–10]. The origin of this band is described as the ≡Si–OH vibration from the defect silanol groups which are produced upon substitution of titania (or other metal oxide species) into the silicalite matrix, but is related to the –OH vibration at 3748 cm^{-1}. Since the 960 cm^{-1} band is not affected by deuterium exchange in TS-1, this is not associated with Si–OH [8]. Hence, this band, common to many Ti-, V-, Mo- and Sn-silicates, could have its origin in $Si-O^- \cdots M^+$ vibration and indicates the possibility of Si–O–M bond formation during hydrothermal synthesis. In silastannoxanes of the type, $R_3Sn-O-SiR'_3$, an intense IR band observed at 950–980 cm^{-1} is associated with the asymmetric stretching vibration of the Si–O–Sn group [11]. We have also observed a clear shift of the wave number of the T–O–T lattice vibration towards lower values with increasing tin content per unit cell. An analogous shift observed for MFI type metallo-silicates has been attributed to the incorporation of the heteroatom in the MFI framework [12].

The UV-Vis DR spectra of Sn-ZSM-12 samples exhibit a characteristic charge-transfer band at about 205 nm in addition to a very small absorption band at around 240 nm (fig. 3, curve a), indicating that most of the Sn^{4+} ions are incorporated in the silicalite network of ZSM-12 probably in a tetrahedral environment.

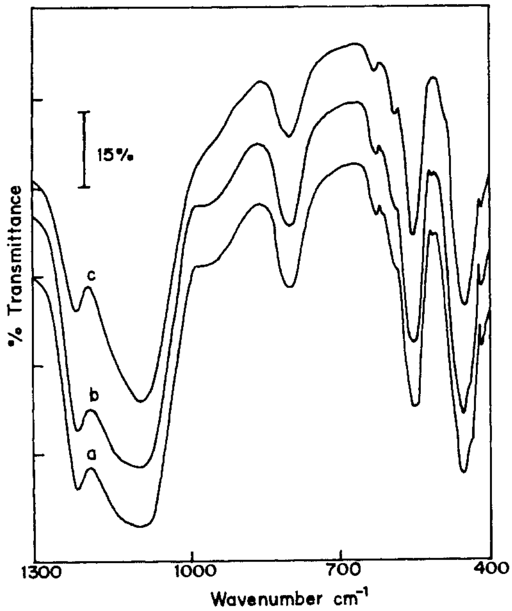

Fig. 2. Framework FT-IR spectra of Sn-ZSM-12 samples (sample A, curve a and sample B, curve b) and Si-ZSM-12 (curve c).

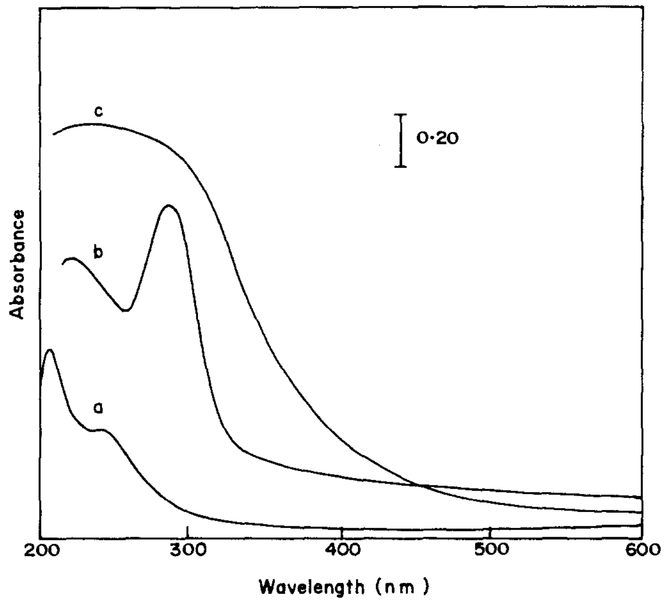

Fig. 3. UV-Vis diffuse reflectance spectra of Sn-ZSM-12 (sample A, curve a), Sn-impregnated Si-ZSM-12 (curve b) and bulk SnO_2 (curve c).

The UV-Vis spectra of Sn-impregnated Si-ZSM-12 and bulk SnO_2, on the other hand, show absorptions at higher wavelengths (285–300 nm) (fig. 3, curves b and c, respectively) due to hexa-coordinated Sn species or polymeric Sn–O–Sn units.

The ^{119}Sn solid state MAS NMR spectra of the Sn-ZSM-12 samples were recorded in a Bruker 300 MHz instrument. The ^{119}Sn MAS NMR signal of the complex (TEOS + $SnCl_4$) in the gel (before crystallization) was observed in the range of −622 to −675 ppm with respect to Me_4Sn. After crystallization, Sn-ZSM-12 samples show a resonance peak at above −650 ppm suggesting the presence of octahedral tin in the samples [3,4]. ^{119}Sn MAS NMR spectra of pure SnO_2 and Sn-impregnated MTW silicalite show a sharp resonance band at −604 ppm. It is possible that a second, minor phase of octahedral tin is present in this material. On the other hand, Sn^{4+} ions either in substitutional, corner- or edge-sharing positions of the silicalite structure or linked to the defect silanols tend to assume five- or six-fold co-ordination with ligands such as -OH or H_2O very easily due to its bigger size. Indeed, on hydration Sn-MFI samples show CT absorptions at 225 and 255 nm, which have been assigned to penta- and hexa-coordinated Sn^{4+} [13]. Further detailed work on ^{119}Sn NMR and Sn Mössbauer would shed more light on this question.

The scanning electron micrographs (Jeol, 5200 model) of Sn-ZSM-12 showed star-like aggregates of needle-shaped crystals of 0.5 × 8 μm size. The Si-ZSM-12 sample consisted of rod-like crystals of 1.0 × 12 μm dimension.

The N_2 adsorption isotherms of Sn-ZSM-12 samples at liquid N_2 temperature

(Omnisorb 100 CX analyser) are characteristic of microporous materials. The BET surface areas of Sn-ZSM-12 samples are in the range of 300–321 $m^2\ g^{-1}$, slightly higher than that of Al-ZSM-12 (280 $m^2\ g^{-1}$, table 1). The amounts of *n*-hexane, cyclohexane and mesitylene adsorbed by Sn-ZSM-12 samples at 298 K and at $p/p_0 = 0.5$ (Cahn electrobalance) are comparable with those of Sn-free ZSM-12 silicalite (table 1) and suggest that the micropores are maintained and that occluded SnO_2-type species is not present in these samples. When Sn-ZSM-12 samples were treated with 5 N HCl for 24 h at 298 K, no detectable Sn was found in the filtrate. Since Sn^{2+} ions are soluble in HCl, the presence of any clustered Sn^{2+} species could also be ruled out.

3.2. CATALYTIC PROPERTIES IN OXIDATION REACTIONS

Catalytic activity is often indicative of the location (framework vs. extra-framework) of the substituted elements in silicalite structures [14]. The results of the oxidation/hydroxylation of various organic compounds including phenol, *m*-cresol and *m*-xylene over Sn-ZSM-12 sample (sample A) are summarised in table 2. Under similar conditions, the Sn-free Si-ZSM-12 sample does not exhibit any cat-

Table 2
Catalytic oxidation using aqueous H_2O_2 over Sn-ZSM-12 [a]

Substrate	Substrate conv. [b] (mol%)	H_2O_2 sel. [c] (mol%)	Product distribution (mol%)	
phenol [d]	16.2	50.6	para-benzoquinone	4.5
			catechol	57.7
			hydroquinone	37.8
m-cresol [e]	19.9	73.5	2,5-dihydroxytoluene	37.0
			3,4-dihydroxytoluene	25.0
			3-hydroxybenzyl alcohol	8.5
			3-hydroxybenzaldehyde	26.3
			others	3.2
m-xylene [f]	15.9	68.5	2,4-dimethylphenol	13.4
			2,6-dimethylphenol	6.4
			3-methylbenzyl alcohol	21.0
			3-methylbenzaldehyde	49.0
			others	10.2

[a] Reaction conditions: catalyst/substrate = 10, 15 and 20 wt% in the case of phenol, *m*-cresol and *m*-xylene, respectively (Si/Sn = 73); substrate/H_2O_2 (mole) = 3; temp. = 353 K; solvent/substrate (mole) = 20; reaction time = 16 h.

[b] Mol% of substrate converted in the formation of all products.

[c] Mol% of H_2O_2 consumed in the formation of all products excluding higher boiling oxygenates not identified and grouped as others.

[d] Solvent H_2O.

[e] Solvent H_2O : acetonitrile (wt) = 3 : 1.

[f] Solvent = acetonitrile; temp. = 373 K; in pressure reactor.

alytic activity in these reactions. Sn(IV)-impregnated ZSM-12 shows only negligible activity in phenol hydroxylation and no activity in the other two reactions.

Sn-ZSM-12 samples exhibited quite high catalytic activity in the hydroxylation of phenol (table 2). The ortho to para products ratio of 1.4 indicates that Sn^{4+} species, responsible for the catalytic activity are isolated and well dispersed on the surface as well as in the bulk of the catalyst. In the oxidation of *m*-cresol, the product selectivity shows that the hydroxylation of the aromatic ring leading to the formation of 2,5- and 3,4-dihydroxytoluenes is predominant (62%) and the oxyfunctionalization of the methyl substituent leads to 3-hydroxybenzyl alcohol and its secondary oxidation product, 3-hydroxybenzaldehyde (34.8%). Even in the hydroxylation of the aromatic nucleus, the para isomer (2,5-dihydroxytoluene) is more (37%) than the ortho isomer (25%). This suggests that the hydroxylation reaction proceeds within the channels of the unidimensional ZSM-12 structure. The ability of the Sn-silicates in the oxyfunctionalization of the methyl substituent in toluene has earlier been observed on Sn-MFI and Sn-MEL samples [3,4].

In contrast to the results obtained in the case of *m*-cresol, the product distribution in *m*-xylene oxidation (table 2) shows that the oxidation of the side chain is preferred to aromatic ring hydroxylation. 3-methylbenzyl alcohol (21 mol%) and its secondary oxidation product, 3-methylbenzaldehyde (49 mol%) are the predominant products (total, 70 mol%), whereas the products of ring hydroxylation, viz., 2,4- and 2,6-dimethylphenols constitute only 20 mol% of the products. The aromatic ring hydroxylation is believed to be an electrophilic substitution reaction proceeding via an ionic mechanism on metallo-silicates [15,16]. The higher electron donating character (+M effect) of the –OH group in *m*-cresol compared to the +I effect of the $-CH_3$ group in *m*-xylene may be responsible for the observed difference in the product distributions. The probability of either of the $-CH_3$ groups undergoing oxidation simultaneously in *m*-xylene is twice that in *m*-cresol and the results reflect exactly such a course of the oxidation reaction. The oxyfunctionalization of the side chain carbon atom along with aromatic ring hydroxylation is a characteristic feature of Sn-silicate molecular sieves. In this respect, Sn-ZSM-12 is similar to the large pore vanadium silicate molecular sieve, V-NCL-1 reported earlier [17].

These results support the view that the hydroxylation of the aromatic ring (with H_2O_2 as oxidant) over Sn-ZSM-12 follows an ionic mechanism, whereas the side chain oxidation occurs predominantly by a radical pathway, as suggested for similar reactions on V-silicate molecular sieves [18].

4. Conclusions

Crystalline microporous tin silicates (Si/Sn>70) with the MTW (ZSM-12) structure have been synthesized using a new diquarternary ammonium template, 1,6-hexamethylene bis(benzyl dimethyl ammonium hydroxide). Unit cell expansion, IR data and UV-Vis absorption data indicate significant incorporation of Sn^{4+} in the MTW framework. Sn-ZSM-12 catalyzes the hydroxylation of phenol, *m*-cresol and *m*-xylene with aqueous H_2O_2.

Acknowledgement

The authors thank Dr. M.K. Dongare for his help in the preparation of the template. NKM and AB are grateful to CSIR, New Delhi, for research fellowships.

References

[1] F.G. Dwyer and E.E. Jenkins, US Patent 3,941,871 (1976).
[2] M. Constantini, J.L. Guth, A. Lopez and J.M. Popa, Euro Patent 466,545 (1992).
[3] N.K. Mal, V. Ramaswamy, S. Ganapathy and A.V. Ramaswamy, J. Chem. Soc. Chem. Commun. (1994) 1933.
[4] N.K. Mal, V. Ramaswamy, S. Ganapathy and A.V. Ramaswamy, Appl. Catal. A (1995), in press.
[5] R.B. LaPierre, A.C. Rohrman, J.L. Schlenker, J.D. Wood, M.K. Rubin and W.J. Rohrbaugh, Zeolites 5 (1985) 347.
[6] A. Bhaumik, M.K. Dongare and R. Kumar, Microporous Materials, submitted.
[7] D.W. Breck, *Zeolite Molecular Sieves* (Wiley, New York, 1974).
[8] G. Deo, A.M. Turek, I.E. Wachs, D.R.C. Huybrechts and P.A. Jacobs, Zeolites 13 (1993) 365.
[9] M.A. Camblor, A. Corma and J. Perez-Pariente, J. Chem. Soc. Chem. Commun. (1993) 557.
[10] P.R. Hari Prasad Rao, A.V. Ramaswamy and P. Ratnasamy, J. Catal. 137 (1992) 225.
[11] H. Schmidbaur, Angew. Chem. Int. Ed. 4 (1965) 201.
[12] G. Vorbeck, J. Hanchen, B. Parlitz, M. Schneider and R. Fricke, J. Chem. Soc. Chem. Commun. (1994) 123.
[13] N.K. Mal and A.V. Ramaswamy, J. Mol. Catal., submitted.
[14] G. Perego, G. Bellusi, C. Corno, M. Taramasso, F. Buonomo and A. Esposito, Stud. Surf. Sci. Catal. 28 (1986) 129.
[15] D.R.C. Huybrechts, P.L. Buskens and P.A. Jacobs, J. Mol. Catal. 71 (1992) 129.
[16] J.S. Reddy, S. Sivasanker and P. Ratnasamy, J. Mol. Catal. 71 (1992) 373.
[17] K.R. Reddy, A.V. Ramaswamy and P. Ratnasamy, J. Chem. Soc. Chem. Commun. (1992) 1613.
[18] A.V. Ramaswamy and S. Sivasanker, Catal. Lett. 22 (1993) 239.